Available online at www.sciencedirect.com
SCIENCE DIRECT®
Physica C 391 (2003) 265–271
PHYSICA C
www.elsevier.com/locate/physc

# Recent developments in processing and performance of hot stacked-sinter forged Bi2223 ceramics

J.G. Noudem *, E. Guilmeau, D. Chateigner

*CRISMAT-ENSICAEN, 6 Boulevard du Maréchal Juin, 14050 Caen Cedex, France*

Received 6 December 2002; received in revised form 14 March 2003; accepted 18 March 2003

**Abstract**

Bulk-textured Bi2223 superconductors with high density have been successfully formed by the hot stacking-forging process. The grain orientation was verified by textural analysis, scanning electron microscopy observation and the critical field deduced from magneto-resistivity measurements.

Transport critical current data of the textured superconductor samples were obtained using DC-measurements. According to current–voltage curves, the transition between the superconducting state and the flux-flow regime corresponds to a high transport critical current density ($J_c$) up to $2 \times 10^4$ A/cm$^2$ at 77 K in a self-field. In addition, $J_c$, values were measured at various temperatures and different applied magnetic fields. Several textured pieces were hot-stacked under various applied stresses. This procedure leads to an increase of the sample thickness and the nominal engineering critical current ($I_c$) in order to use textured-Bi2223 for practical power generation.


*PACS:* 74.72.Hs; 74.10.+v; 74.25.Fy; 74.25.Ha; 74.72.–h; 74.62.Bf
*Keywords:* Bi2223; Hot forging; Stacking/joining; Texture analysis; Electrical properties

## 1. Introduction

The failure of conventional devices in limiting high fault currents has led to the exploration of superconducting materials for fault current limiters (FCL). The existing superconducting FCLs can be classified into two types, resistitive [1–5] and inductive [6,7]. The advantages and disadvantages of both types have been extensively discussed [1–7]. In particular, these concern the availability and ease of formation of the superconducting materials into desired structures [8,9], for which the ability to create superconducting materials with a suitable shape is one of the important parameters in the design of FCLs.

So far, the superconducting materials studied for use as FCLs are Bi-system and Y123. The ease of shape processing of Bi-based superconductors makes them suitable for the design of inductive type FCLs. Resistive type FCLs utilize long-length superconductors as resistive elements. The difficulty in processing bulk or thin films of Bi-materials into such lengths without metallic sheaths or undesirable substrates, in front of the capability of achieving large-area, high $J_c$ Y123 films, led to the

* Corresponding author. Tel.: +33-231-452915; fax: +33-231-951600.
*E-mail address:* noudem@ismra.fr (J.G. Noudem).

0921-4534/$ - see front matter © 2003 Elsevier B.V. All rights reserved.
doi:10.1016/S0921-4534(03)00934-1

design of resistive FCLs with using the Y123 family of superconducting materials.

Although the Y123 thin films, to some extent, are acceptable for small-scale FCLs, behave disadvantageously in some cases. One of their important limitations is the low engineering current ($I_c$) that they can tolerate, in spite of their higher $J_c$s compared to bulks. Unfortunately, $I_c$s do not increase linearly with increasing film thickness, because of the intrinsic limitation of thin film processing techniques in maintaining the epitaxial texture induced by the underlying substrate beyond one micrometer of thickness. It results that $J_c$s degrades exponentially with increasing thicknesses. Another disadvantage is the low potential of thin films to withstand Joule's heating during fault currents, even if their low thermal inertia compared to melt-textured bulk Y123 materials acts favorably. Moreover, the properties of film substrates also hinder at times the performance of thin films.

The important material characteristics for resistive type FCLs can be listed as follows:

- exhibition of a high $I_c$,
- capability to absorb the dissipated energy before the line circuit breaker opens without any damage,
- rapid extraction of heat during hot spot formation.

Recently we have modified the starting precursors of Bi2223 and improved the densification, texturation and $J_c$ of the Bi2223 compounds [10,11]. These resulting properties imply that Bi2223 sinter-forged bulks could be potential candidates for resistive FCLs, especially since some studies [1,12] show that high $J_c$ is favorable to the normal state transition during the quench tests.

In this paper, the potentiality of formation of stacked textured Bi2223 for use as a resistive FCL is explored by studying the preliminary electrical characteristics, $T_c$, normal state resistivity, and $J_c$.

## 2. Experimental

The details of the preparation process of Bi2223 bulk-textured materials by thermomechanical processing are reported elsewhere [11]. Briefly, the powder was prepared by the EDTA sol–gel method using the nominal composition $Bi_{1.85}Pb_{0.35}Sr_2Ca_2Cu_{3.1}O_{10+\delta}$. The raw powder was then mixed in an agate ball mill and calcined under air at 820 °C for 24 h. The resulting powder exhibits an assemblage composed mainly of Bi2212 and secondary phases such as $Ca_2PbO_4$, CuO, $Ca_2CuO_4$ and $Sr_{14}Cu_{24}O_{41}$ [13]. The calcined powder was then cold-pressed into pellets of 2 mm thick and 25 mm in diameter under an uniaxial pressure of 23 MPa which gives a green density of 60% of the theoretical one. The pellets were then set in the furnace [14] between two 0.125 mm silver sheets to avoid any reaction with alumina supports under heating. The stress employed was fixed at 10 MPa, the working temperature was fixed at 845 °C and the dwell time is equal to 100 h. The resulting Bi2223 discs have a thickness of 0.2 mm, and demonstrate microstructural features of a dense and textured bulk sample, with the highest texture strengths ever seen in such compounds.

A series of several samples has been elaborated by hot-stacking three of the previous discs in the absence of soldering agents under various uniaxial pressures up to 28 MPa. The same stress and dwell temperature were used, and 20 h of dwelling time was used, resulting in three samples.

The texture was analysed using the full width at half maximum of the distribution densities (FWHD), calculated on the basis of the XRD intensities of the (008)-2212 and (0010)-2223 peaks [11].

Bar-shaped samples, with dimensions of 10–15 mm × 1–3 mm, were cut from the thick samples using a low speed diamond saw. The long axis of the bar was cut perpendicular to the stress axis of the samples. Variable thicknesses in the 0.2–0.56 mm range were obtained according to the pressure level applied during the hot-stacking/joining process. Normal contacts between the samples and current leads were prepared by painting commercial silver paste (Dupont 4929).

The samples were subsequently annealed in flowing 7.5% oxygen and 92.5% nitrogen at 820 °C for 100 h, cooled at 1 °C/h to 800 °C, and then quenched to room temperature. A scanning electron microscope (SEM) was used to investigate the

surface morphology. Electrical properties were measured by standard four-point contacts method, applying a 1 μV/cm criteria for the critical current. The current input was produced by a 120 A/4 V DC-Magnet power supply. The sample was immersed in a liquid nitrogen bath and measured in various external fields. The typical contact resistances were less than 1 $\mu\Omega\,cm^2$ at 77 K. Resistivity measurements, $R(T)$, were performed by PPMS (magnet power supply) in magnetic fields from 0 to 7 T.

## 3. Results and discussion

### 3.1. Microstructure

Fig. 1 shows SEM micrographs of faces broken parallel to the stress axis $\sigma$ for a magnification showing individual platelets of a single sinter-forged disc (Fig. 1a) and a lower magnification illustrating an ensemble of three hot-stacked discs (Fig. 1b). The initial single disc shows a high degree

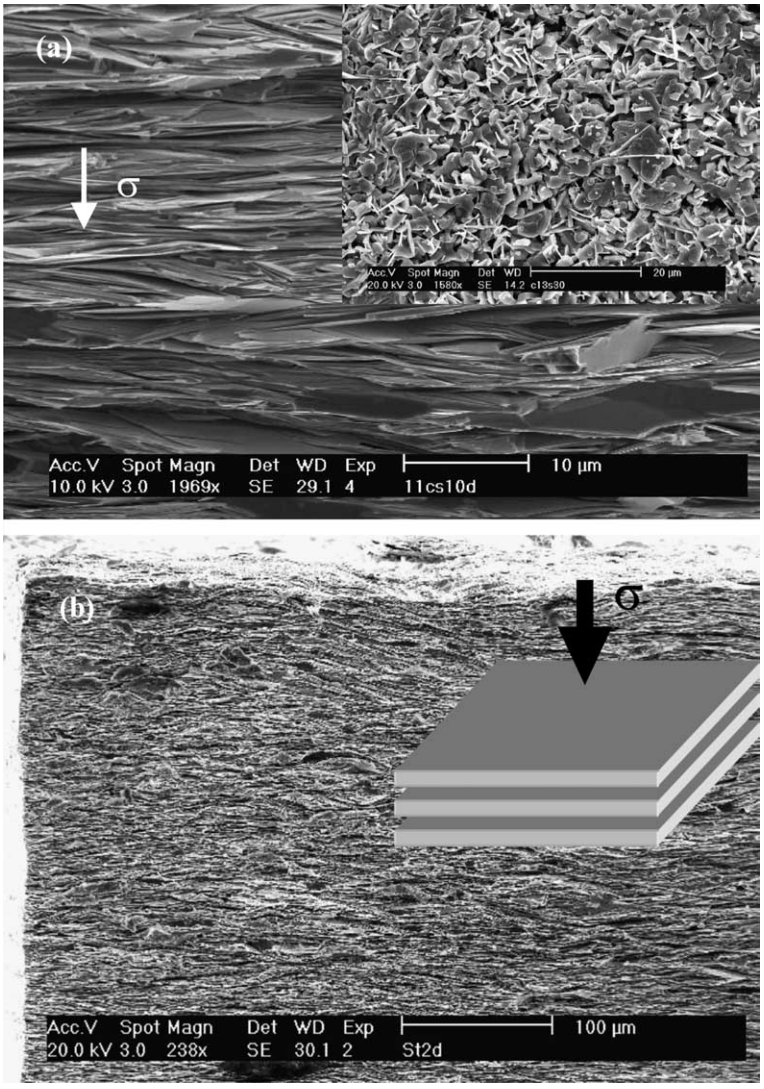


Fig. 1. (a) SEM micrograph of a single sinter-forged sample showing the platelets alignment perpendicularly to the stress direction. Inset shows a standard sinter sample without applied stress. (b) Cross sectional view of the stacked ceramics, the total thickness is around 400 μm.

of orientation of the large platelets compactly stacked up with their mean normals aligned along the stress direction, in contrast with the sample processed without stress (inset of Fig. 1a), in which much smaller platelets appear to be randomly distributed and loosely assembled. The internal alignment of the platelets in the initial discs is not perturbed by the new hot-stacking procedure (Fig. 1b) and the morphology of the stacked sample shows the dense ceramic with the formation of aligned platelets along the whole thickness stack. Interestingly, we cannot distinguish any interface between the initial discs in the hot-stacking processed sample at this scale, which would favor the microstructural and physical properties homogeneity throughout the thickness of the whole stack. In the present case, the thickness of the sample (Fig. 1b) is measured to be 400 μm, but can be varied from 200 to 600 μm by varying the value of the applied pressure, although this thickness may be increased furthermore.

### 3.2. Resistivity

In Fig. 2, the temperature dependence of the resistivity is shown for several magnetic fields up to 7 T applied perpendicular (Fig. 2a) and parallel (Fig. 2b) to the mean $c$-axis of the textured material. The transition to the superconducting state typically shifts to lower temperatures for increasing applied magnetic fields and when these latter are applied perpendicular to the $(a, b)$ planes of the structure, with a maximum critical temperature of $T_c \approx 107$ K in self-field.

From the magnetoresistance curves, $T_{coff}$, defined as the disappearance of resistivity or the appearance of an electrical resistance and dissipative effects, can be used to determine the critical line $H_c$ (T). This line has been determined at 10% $\rho_n$, where $\rho_n$ is the normal state resistance above the transition. Fig. 2c shows critical field versus critical temperature curves deduced from Fig. 2a and b and corresponding to the above-mentioned criterion. The anisotropy ratio $H_c^{\perp c}/H_c^{\parallel c}$ has a value of about 7.5 at 77 K, indicative of crystallite alignment and correlated to the SEM microstructure observations and texture analysis described below.

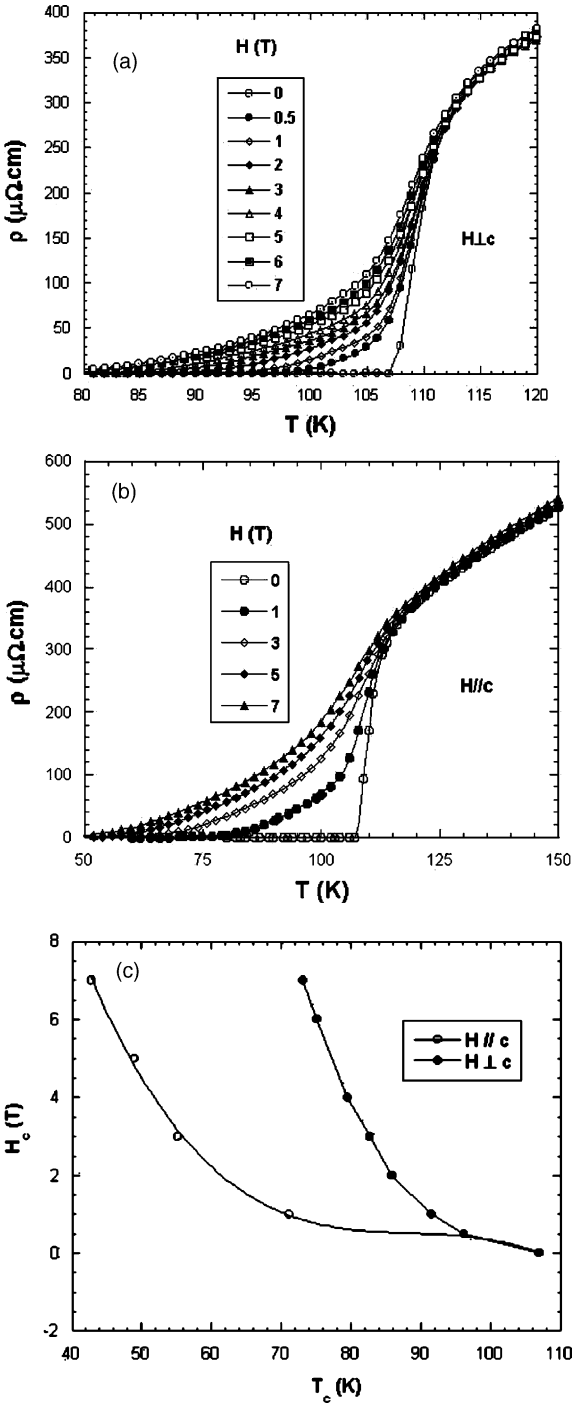


Fig. 2. Temperature dependence of the electrical resistance under various applied magnetic fields, $H$. (a) $H \perp c$, (b) $H \| c$, (c) phase diagram showing the critical field-$H_c$ versus the critical temperature-$T_c$ deduced at 10% of normal state resistance.

### 3.3. Critical current measurements and textural analysis

Direct transport $J_c$ measurements were performed firstly on the bar samples obtained from a typical single disc. The field dependence of the critical current density is shown in Fig. 3 for 65 and 77 K. From the typical *E–I* curve, and according to the transition between the fully superconducting state and the flux-flow regime, the transport critical current can be measured about 40 A at 77 K and 0 T, corresponding to a self-field critical current density of $2.1 \times 10^4$ A/cm$^2$ using a 1 μV/cm criteria. According to the sample dimensions (cross section of $0.24 \times 1.06$ mm$^2$ and voltage taps of 6 mm), the resistivity value of 250 μΩ cm has been deduced above $J_c$ at 5 μV/cm. The temperature dependence of $J_c$ is also shown in Fig. 3. $J_c$ improves markedly as the temperature falls from 77 to 65 K. The critical current density is enhanced by 50% and reaches $3.9 \times 10^4$ A/cm$^2$ at 65 K, 0 T. It is clear that $J_c$ is sensitive to the applied field and decreases with increasing magnetic field, but the value of ≈3000 A/cm$^2$ at 77 K in 1.5 T is slightly higher for the BSCCO system because the grain boundaries of this compound are very sensitive under magnetic field. This may be due to the processing method, since the intergranular medium has been modified by the strong connection between platelets resulting from the achievement of a high degree of texture, inducing dense samples and reducing the number of grain boundaries (Fig. 1). The maximum $J_c$ value obtained at 77 K is comparable with some results obtained on Bi2223 powder in tube (PIT) samples and reported in the literature [15,16]. But the largest reported value of 50 kA/cm$^2$ was measured in a PIT specimen [17] of a few tens of micrometers thick, not suited for potential high nominal current transports. Moreover, in such silver sheathed tapes, surface pinning may favor much higher critical current density, which would vanish for larger thicknesses with less surfacic phenomena.

For high power applications, the nominal $I_c$ should be as high as possible. To obtain a high $I_c$, several single discs (25 mm diameter) were shaped in 15 mm × 15 mm on side and then stacked thermomechanically under various uniaxial stresses. Several bars from each hot-stacked sample were prepared for current and texture measurements. Fig. 4 shows the $J_c$ and crystallite distribution values (FWHD) versus uniaxially applied stress during the heat treatment. One can note, (i) the dispersion of $J_c$ from bar to bar cut in each sample (same applied stress), (ii) the $J_c$ increase with increasing stresses up to a maximum around 20 MPa and (iii) the correlated decrease of the FWHD of both superconducting phases with increasing the stress with a minimum also around 20 MPa. The dispersion of $J_c$ from bar to bar is not

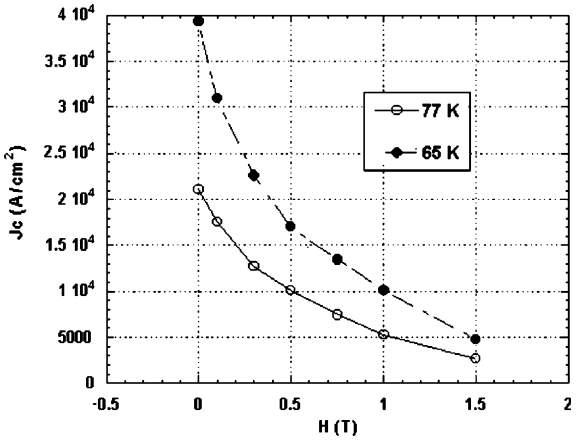


Fig. 3. $J_c$ versus magnetic field for hot-forged single disc at 77 and 65 K.

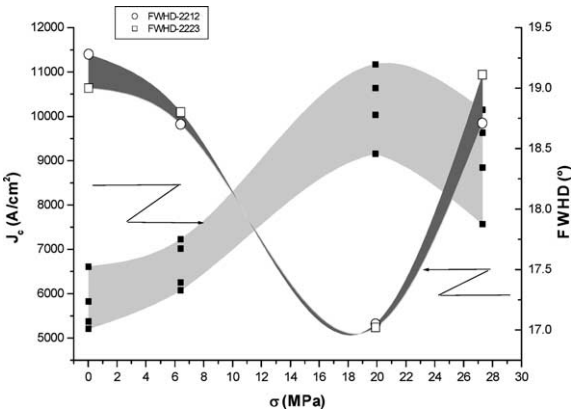


Fig. 4. Critical current density at 77 K and self-field of hot-stacked samples showing the $J_c$s-area and FWHDs versus applied stress.

believed to come from sample inhomogeneities neither in compositions nor pressure or texture, since we did not notice regular $J_c$ variations with the location of the bar in the sample, i.e. distance from the center to the disc. This dispersion may be alternatively caused either by microscopic cracks induced during the treatment or during cutting, or by the self-field at the surface of the superconductor. Both of these local effects remain more or less uncontrolled in the process and express the deviation at the scale of the $J_c$ measurements, which is rarely evidenced in the literature. The inverse trend of the $J_c$ and FWHD curves is quite interesting. It proves clearly that the transport properties are directly correlated to the texture quality of the forged discs down to FWHDs as low as 17°. The optimal value of applied stress to attain highest critical current densities corresponds also to the optimal one to induce better grain connectivity and alignment, i.e. lower FWHDs. In the process conditions, a reduction of the FWHD of around 2° induces a 100% $J_c$ gain approximately for 20 MPa of applied stress and for FWHDs in the 18° range. It should be noticed that this effect is observed for closely developed textures between the Bi2212 and Bi2223 phases which ensures enough links for the current paths in the compound. These close textures are coming from the nucleation-growth mechanisms between the two phases, which is achieved in the sinter-forging method [11]. We do not have any hint at the moment whether if achieving FWHDs smaller than 14° [18] may still enlarge $J_c$s, but compared to YBCO thin film textural values [19] the ones observed in this work are 4–6 times larger.

We notice that, the maximum $J_c \approx 11$ kA/cm$^2$ in the case of hot-stacking of several pieces is lower than the 20 kA/cm$^2$ previously reported [10] for the optimal sinter-forged discs. This difference is due to the lower sinter-forging time used here, e.g. 20 h with respect to 100 h for the optimal single sample. The resulting Bi2223 phase content is lower and the orientation distributions of the Bi2212 and the Bi2223 phases are broader [18]. However, if we compare $J_c$ values of single and stacked samples using the same thermomechanical history, we note that, $J_c$ values are around 13 kA/cm$^2$ for single discs and 11 kA/cm$^2$ for stacked discs, which are reasonably comparable values in front of the dispersion of $J_c$ values observed from bar to bar.

## 4. Conclusion

From the above results it can be concluded that:

- Single dense and highly textured discs were prepared using the sinter-forging method.
- Hot-stacking without soldering agents has been successfully used to process thick samples up to 0.6 mm.
- The texture degree has been quantified by means of XRD and correlated to the transport current density, $J_c$. Lower FWHDs may give rise to larger $J_c$s.
- A ratio $H_c^{\perp c}/H_c^{\parallel c} \approx 7.5$ at 77 K was found for the single textured sample.
- The transport current density, $J_c$, of sinter-forging single discs was investigated and the highest $J_c$ of $2.1 \times 10^4$ A/cm$^2$ at 77 K and $3.9 \times 10^4$ A/cm$^2$ at 65 K have been measured in 0 T.
- The 0.56 mm thick stacked sample can support reproducibly a nominal $I_c$ of 89 A. This indicates that this material could be a potential candidate for FCL devices. As an intermediate step towards the achievement of FCL, the stacked discs will be cut, shaped (meanders) and assembled in order to build a prototype with high voltage.

Further investigations on hot-stacked samples are under way to improve $I_c$ and to perform the angular dependence of the transport critical current.

## Acknowledgements

E. Guilmeau is grateful to the «French Ministère de la Recherche et de la Technologie» for his Ph.D. fellowship.

## References

[1] J.G. Noudem, D. Bourgault, J.M. Barbut, P. Tixador, R. Tournier, Physica C 349 (2001) 47.

[2] M. Noe, M.-P. Juengst, F.N. Werfel, M. Baecker, J. Bock, S. Elschner, Inst. Phys. Conf. Ser. No. 167, paper presented at Applied Superconductivity, Spain, 14–17 September 1999, p. 989.
[3] B. Gromoll, G. Reis, W. Schmidt, H.P. Krämer, P. Kummeth, H.W. Neumüller, IEEE Trans. Appl. Supercond. 7 (1997) 828.
[4] M. Morita, O. Miura, D. Ito, Supercond. Sci. Technol. 13 (2000) 896.
[5] R. Tournier, E. Beaugnon, O. Belmont, X. Chaud, D. Bourgault, D. Isfort, L. Porcar, P. Tixador, Supercond. Sci. Technol. 13 (2000) 886.
[6] X. Obradors, T. Puig, E. Mendoza, J. Plain, J. Figueras, X. Granados, A.E. Carillo, E. Vares, F. Sandiumengue, P. Tixador, Supercond. Sci. Technol. 13 (2000) 879.
[7] W. Paul, M. Lakner, J. Rhyner, P. Unternahner, Th. Baumann, M. Chen, L. Widenhorn, A. Guérig, Supercond. Sci. Technol. 10 (1997) 914.
[8] E. Sudhakar Reddy, M. Tarka, G.J. Schmitz, Supercond. Sci. Technol. 15 (2002) 21.
[9] J.G. Noudem, E. Sudhakar Reddy, G.J. Schmitz, Physica C, in press, corrected proof available online since 26 March 2003.
[10] J.G. Noudem, E. Guilmeau, E. Sudhakar Reddy, M. Noe, G.J. Schmitz, presented at ICMC 2002 Xi'an China, Physica C 386 (2003) 202.
[11] E. Guilmeau, D. Chateigner, J.G. Noudem, Supercond. Sci. Technol. 15 (2002) 1436.
[12] J.G. Noudem, J.M. Barbut, O. Belmont, D. Bourgault, J. Sanchez, P. Tixador, R. Tournier, Inst. Phys. Conf. Ser. No. 167, paper presented at Applied Superconductivity, Spain, 14–17 September 1999, p. 1005.
[13] E. Guilmeau, J.G. Noudem, Supercond. Sci. Technol. 15 (2002) 1566.
[14] V. Rouessac, J. Wang, J. Provost, G. Desgardin, Physica C 268 (1996) 225.
[15] K. Venugopal, G. Swaminathan, Cryogenics 34 (1994) 325.
[16] V. Garnier, C. Goupil, G. Desgardin, Supercond. Sci. Technol. 14 (2001) 717.
[17] M. Ueyama, T. Hikata, T. Kato, K. Sato, Jpn. J. Appl. Phys. 30 (1991) 1384.
[18] E. Guilmeau, J.G. Noudem, D. Chateigner, Supercond. Sci. Technol. 16 (2003) 484.
[19] M. Pernet, D. Chateigner, P. Germi, C. Dubourdieu, O. Thomas, J.P. Sénateur, D. Chambonnet, C. Belouet, Physica C 235–240 (1994) 627.